Let-7i Regulates KGN Proliferation and Estradiol Biosynthesis By Directly Targeting IMP2 in Polycystic Ovary Syndrome

Xiao Xu
Obstetrics and Gynecology Hospital of Fudan University
Hao-Ran Shen
Obstetrics and Gynecology Hospital of Fudan University
Min Yu
Obstetrics and Gynecology Hospital of Fudan University
Mei-Rong Du
Obstetrics and Gynecology Hospital of Fudan University
Xue-Lian Li (xllifc@fudan.edu.cn)
OB/GYN Hospital, Fudan University https://orcid.org/0000-0003-2195-7904

Research Article

Keywords: Polycystic ovary syndrome, Granulosa cell, let-7i, IMP2, Proliferation, estradiol biosynthesis

Posted Date: March 17th, 2021

DOI: https://doi.org/10.21203/rs.3.rs-292614/v1

Abstract

Background:

Increased granulosa cell division is associated with abnormal folliculogenesis in polycystic ovary syndrome (PCOS). As the most abundant microRNA molecule in the development of follicles, let-7i was found to be differentially expressed in PCOS patients and controls. This study aimed to investigate the role of let-7i in PCOS and explore its related mechanisms.

Methods: The expression of let-7i was measured in GCs from women with PCOS and without PCOS. An immortalized human granulose cell line, KGN, was used for the functional study. Let-7i mimics, let-7i inhibitors, lentiviruses expressing IMP2 and small-interfering RNA were transfected respectively into KGN cells. KGN cell proliferation was determined by an EdU assay kit and cck-8. Cell cycle and apoptosis were determined by PI staining and flow cytometry analysis. Quantitative real-time polymerase chain reaction (qRT-PCR) and western blotting were utilized to evaluate genes expression. Estradiol biosynthesis was determined by ELISA analysis. Bioinformatics analysis and luciferase reporter assay were applied to confirm the target gene of let-7i.

Results: let-7i was down-regulated in PCOS GCs. Let-7i mimics (150 nM) inhibited KGN proliferation, arrested cell cycle progression, and decreased aromatase expression and estradiol production, while the let-7i inhibitors (150 nM) had the opposite effect. Bioinformatics analysis and qRT-PCR identified IMP2 was a target of let-7i. QRT-PCR and western blot analysis indicated that IMP2 was up-regulated in PCOS GCs and the expression of IMP2 was suppressed by let-7i in KGN. The further luciferase reporter assay combined with rescue assay validated that let-7i inhibited KGN proliferation and estradiol production by directly targeting IMP2 mRNA.

Conclusions: Let-7i was down-regulated in PCOS GCs. Let-7i overexpression inhibited KGN proliferation and decreased estradiol production in an IMP2-dependent manner, providing insights into the pathogenesis of PCOS.

Background

Polycystic ovary syndrome (PCOS) is not only one of the most common reproductive endocrine disorders, but also a main cause of anovulatory infertility, affecting 5 to 20% of women of reproductive age (1). It is characterized by ovulatory dysfunction, polycystic ovaries and androgen excess (2) (3). Women with PCOS have an increased risk of developing infertility, metabolic abnormalities, endometrial cancer and cardiovascular events. The etiology of PCOS includes genetic factors, environmental influence and epigenetic changes (4). The exact mechanism of ovarian dysfunction and disordered steroidogenesis in PCOS is not fully understood. Compared with women without PCOS, PCOS patients have more small growing follicles, high granulosa cells (GCs) proliferation and low GCs apoptosis (5, 6). Abnormal GCs proliferation play a part vital role in pathogenesis of PCOS by interfering with steroidogenesis, follicular

development, and oocyte maturation (7, 8). Therefore, exploring the underlying molecular mechanism of GCs dysfunction would provide a new understanding in the pathogenesis of PCOS.

MicroRNAs (miRNAs) are a group of small non-coding RNAs that are involved in mediating RNA destabilization and/or inhibiting translation by binding partially complementary target mRNAs. The role of miRNA has been reported in regulating GCs function, oocyte maturation, follicle development and abnormal steroidogenesis in PCOS (9–13). Aberrant expression of miRNAs in GCs may contribute to the pathology of PCOS. Lethal-7 (let-7) miRNA family, including let-7a (-1, -2 and − 3), let-7b, let-7c, let-7d, let-7e, let-7f (-1 and − 2), let-7g, let-7i, and miRNA-98 in human (14), was found to be the most commonly abundant miRNAs cluster in the ovary (15). Let-7 family has been widely reported to play a role in tumor repression, lipid metabolism and steroidogenesis (16–18). As a critical regulator governing cellular growth signaling pathway (19), let-7 also regulates GCs growth and ovarian development. In the mammalian ovary, let-7g promotes porcine GCs apoptosis by blocking the transforming growth factor β pathway (20). Ectopic expression of let-7b is involved in partial restoration of abnormal ovarian angiogenesis in the corpus luteum of Dicer hypomorphic mice (21). In the family of let-7, let-7i is the most abundant miRNA identified in bovine oocyte and GCs from different staged-follicles (22). Let-7i expression was decreased in atretic follicles as compared to that in healthy follicles (23) and was significantly up-regulated in follicle activation (24). A recent study showed that the expression of let-7i was significantly different between PCOS patients and controls (25, 26), that suggested the potential role of let-7i in the pathogenesis of PCOS.

In this study, we explored that the expression of let-7i was down-regulated in GCs of PCOS patients. Also, we assessed the role of let-7i in GC proliferation and steroidogenesis and further explored its potential mechanism. We found the potential target of let-7i performed by bioinformatic analysis, which predicted that insulin-like growth factor 2 mRNA binding protein (IMP) 1–3 belonging to IMP family might be the targets of let-7i. IMP family serves as the RNA-binding protein, regulating mRNA localization, stability and translation (27). Compared with IMP1 and IMP3, IMP2 is the most widely expressed in oocytes and GCs of growing follicles among three paralogs, and participates in oocyte development (28), ovulation (29) and embryo implantation (30). Crucially, a recent study has found that the expression of IMP2 was overexpressed in PCOS patients as compared to that in non-PCOS patients, and up-regulated expression of IMP2 promoted abnormal GCs proliferation by stabilizing the mRNA of proliferation-related genes (31) in PCOS. We confirmed that the expression of IMP2 was up-regulated in GCs of PCOS patients. We further explore that the effects of let-7i on GCs proliferation by targeting IMP2 in GCs. Our findings provide a new molecular mechanism in PCOS disease.

Methods

Clinical samples

We recruited twenty-four patients with and without PCOS who were undergoing in vitro fertilization-embryo transfer/intracytoplasmic sperm injection (IVF-ET/ICSI) at Shanghai Jiai Genetics and IVF

Institute, in the period from January to June 2019. The Human Research Ethics Committee of the Obstetrics and Gynecology Hospital of Fudan University approved the study. Eleven patients were diagnosed as PCOS according to the Rotterdam revised criteria (32) (2 out of 3): oligo- or anovulation; clinical and/or biochemical signs of hyperandrogenism; and polycystic ovaries with exclusion of other etiologies (congenital adrenal hyperplasia, androgen-secreting tumors, Cushing's syndrome). Thirteen participants, forming the non-PCOS group, were recruited because tubal factor infertility or male factor, who regular menstrual cycles (26-35 days), normal ovarian morphology and no clinical or biochemical evidence of hyperandrogenism. Patients with genetic diseases, thyroid diseases, a family history of type 2 diabetes mellitus within 3 months before the recruitment were excluded. Follicular fluid and granulosa cells from such patients were usually collected as clinical samples for the study of PCOS disease (33, 34). The clinical characteristics of PCOS and non-PCOS group women are shown in the **Table 1**.

Isolation of human GCs

Human GCs were collected from PCOS and non-PCOS patients undergoing IVF/ICSI. Oocyte retrieval was performed under the guidance of the transvaginal ultrasonography after human chorionic gonadotropin administration. After oocyte retrieval, follicular fluid was centrifuged at 2000 rpm for 10min, the precipitates were digested with hyaluronidase (80 IU/ml) (Sigma, St. Louis, Mo., USA) for 30 min at 37℃, then transferred into lymphocyte separation medium (LTS1077-1; TBD, Tianjin, China) and centrifuged at 1500 rpm for 10 min (35). GCs were isolated from the interface layer, then washed and resuspended in phosphate buffer saline (PBS) (GNM10010; Genom, Hangzhou, China). Owing to the difficulties in obtaining human sufficient quantities of GCs and in maintain primary cultures, fresh GCs cells were used for RNA or protein extraction immediately after pufification.

Cell culture

We used an immortalized human GCs line KGN for functional studies. The KGN cell line is a steroidogenic human granulosa-like tumor cell line. KGN cells were obtained from Shandong University and were cultured with phenol red–free DMEM/F12 (GNM11039; Genom) supplemented with 10% fetal bovine serum (10270-106; Gibco, NY) and 1% penicillin-streptomycin (C125C5; NCM, Suzhou, China) (36). KGN cells were cultured in a humidified atmosphere (5% CO_2) at 37℃ and digested with 0.25% trypsin (containing EDTA) (GNM25200; Genom) when passaged.

Bioinformatics analysis

Potential target genes of let-7i (let-7i-5p) were predicted by three databases: Starbase (http://starbase.sysu.edu.cn/), Mirwalk (http://zmf.umm.uni-heidelberg.de/apps/zmf/mirwalk2/), and TargetScan (http://www.targetscan.org). There are 116 genes overlapping in all three databases. We evaluated the binding site strength. IMP1-3 were unverified targets with high binding scores.

Vector construction and transfection

Lentiviruses expressing IMP2 (lenti-IMP2) (31592-1; GeneChem, Shanghai, China) and the control lentiviruses (lenti-ctrl) (CON335; GeneChem) were transfected respectively into KGN cells at 70-80% confluency of cells using HiTransG P reagent (GeneChem). Puromycin (REVG1001; GeneChem) was used to select stably transfected clones according to the manufacturer's protocol. Small interfering RNA (si-RNA) targeting IMP2 (si-IMP2) and siRNA control (si-ctrl) were purchased from GenePharma (Shanghai, China). Si-IMP2-1 (si-1) sequence (5'-3'), GCGAAAGGAUGGUCAUCAUTT; si-IMP-2 (si-2) sequence, ACAGGACUGUCCGUGCUAUTT; si-IMP2-3 (si-3) sequence, GCUGUUAACCAACAAGCCATT. let-7i mimics (miR10000415, micrONTM hsa-let-7i-5p mimic), mimics-negative control (mi-ctrl) (miR1N0000001, micrON mimic NC #22), let-7i inhibitors (miR20000415, micrOFFTM hsa-let-7i-5p inhibitor), inhibitors-negative control (in-ctrl) (miR2N0000001, micrOFF inhibitor NC #22) were purchased from RiboBio Co., Ltd (Guangzhou, China). SiRNA (100nM), miRNA mimics (150nM), mi-ctrl (150nM), miRNA inhibitors (150nM) and in-ctrl (150nM) were transfected respectively into KGN cells at 40-50% confluency of cells using Lipofectamine 3000 (l3000015; Invitrogen, CA) according to the manufacturer's protocol. After transfection for 48h, the cells were collected for further investigations.

RNA extraction and quantitative real-time polymerase chain reaction

Total RNA from human GCs or KGN cells was extracted using the TRIzol reagent (9109; TaKaRa, Dalian, China). 1mL of TRIzol reagent was added gently to each well of 6-well plate. The concentration and quality of all the RNA samples were evaluated using a NanoDrop 2000 spectrophotometer (Thermo Fisher Scientific), and the 260/280 values for all of samples were above 1.8 and 1.9. To measure mRNA or miRNA expression, RNA (1 μg) was then reverse transcribed using the PrimerScript^{TM} RT reagent Kit (RR037A, TaKaRa) in a 10μl reaction volume. Quantitative real-time polymerase chain reaction (qRT-PCR) was performed using TB Green Premix Ex Taq^{TM} II (RR820B, TaKaRa). Let-7i levels were measured by qRT-PCR using Bulge-Loop hsa-let-7i-5p Primer Set (MQPS0000414; Ribobio) with U6 small nuclear RNA (MQPS0000002; Ribobio) as an internal control. Other genes' expression was normalized to GAPDH. Each sample was run in triplicate. Data were analyzed according to $2^{-\Delta\Delta Ct}$ method. The primer list is included in the **Table 2.**

Protein extraction and western blotting analysis

Human GCs and KGN cells were lysed on ice in radioimmunoprecipitation assay lysis buffer (P0013B; Beyotime, Haimen, China), supplemented with the protease inhibitor cocktail (HY-K0010, HY-K0021, HY-K0022, MedChemExpress, Monmouth Junction, NJ, USA) of 1mM each. After centrifugation at 12,000g for 30min, protein concentrations were quantified using a bicinchoninic acid protein assay kit (P0010; Beyotime). Equal amount of protein was separated by sodium dodecyl sulfonate polyacrylamide gel and electro-transferred to polyvinylidene difluoride membrane (IPVH00010; Millipore, Billerica, USA). After blocking with 5% non-fat milk for 2 h at room temperature, membranes were incubated with anti-IMP2 (1:2000, ab124930; Abcam, Cambridge, UK), anti -Aromatase (1:1000, ab18995; Abcam) and anti-GAPDH antibodies (1:10000, ab181602; Abcam) respectively overnight at 4℃ and were washed by 0.1% TBST. Then, the membrane was incubated with horseradish peroxidase–conjugated anti-rabbit secondary

antibodies (1:5000, SA00001-2, Proteintech) for 1 h at room temperature. Protein expression was determined using an enhanced chemiluminescence detection system (General Electric Company, Fairfield, USA).

5-ethynyl-2'-deoxyuridine incorporation assay

According to the manufacturer's instructions, Cell-Light^{TM} EdU Apollo567 In Vitro Kit (C10310-1; Ribobio) was used for cell proliferation assay. For 5-ethynyl-2'-deoxyuridine (EdU) assay, KGN cells were cultured in 96-well plates at a density of 3×10^3 per well. At 48h after transfection with let-7i mimics or let-7i inhibitors or corresponding controls, 50 μM EdU labeling medium was added to the cell culture and incubated for 2 h at 37°C with 5% CO_2. Then, the cells were fixed with 4% paraformaldehyde for 30 min, incubated with 2mg/ml glycine (50 μl per well) for 5 min. After being washed with PBS, the cells were permeabilized with 0.5 % Triton X and treated with 1×Apollo solution for 30 min at room temperature in the dark. The cells were incubated with 100 μl 1×Hoechst 33342 solution for 30 min at room temperature in the dark and then washed with PBS. Finally, the images were captured with a fluorescence microscopy (Olympus, Tokyo, Japan) and the ratio of EdU-positive cells to Hoechst-positive cells was calculated from five random fields in three wells.

Cell cycle assay

PI/RNase staining buffer solution (550825, BD Pharmingen) was performed to detect nuclear DNA from cell suspensions. KGN cells transfected with let-7i mimics or let-7i inhibitors or corresponding controls were plated in 12-well plates and incubated at 37°C for 48h. Then, the cells were collected and washed with buffer solution three times, and the cell cycle distribution was analyzed using propidium iodide (PI) staining and flow cytometry (BD FACS Calibur, USA). Data were analyzed by Flow Jo v.10.0.7 software.

Cell counting Kit-8 assay

Cell viability was determined using Cell-Counting Kit-8 (CCK-8) (ck04, DOJINDO, Japan). KGN cells transfected with let-7i mimics or let-7i inhibitors or corresponding controls were reseeded in 96-well plates at 1.5×10^3 cells/well in 100 μl cell suspension. 10 μl CCK-8 reagent was added to each well quickly and then the cells were cultured for 1.5 h at 37°C at indicated time points (0, 24, 48, and 72 hours). Optical density was measured at 450 nm using a microplate reader. Each experiment was carried out in triplicate at least.

Apoptosis assay

We used the Annexin V/ PI staining for the analysis of apoptotic cells. 1×10^6 KGN cells transfected with let-7i mimics or corresponding controls were digested with 0.25% trypsin (without EDTA) (GNM15050; Genom) and washed twice with ice-cold PBS. The cells were then stained and treated with the Annexin V PE apoptosis detection Kit (559763, BD Pharmingen) according to the manufacturer's guidelines.

Experiments were performed by flow cytometry (BD FACS Calibur, USA) and data were analyzed by Flow Jo v.10.0.7 software.

Measurement of estradiol levels

KGN cells were seeded in 24-well plates in serum-free and treated with 100 nM testosterone (T) and 1 μM Forskolin (FSK) for 24 h after transfection with let-7i mimics or let-7i inhibitors. T and FSK were purchased from Sigma-Aldrich Co. Ltd. T, as a substrate for aromatase, is converted to E2 under the action of aromatase in GCs (37). Since the expression level of functional FSH receptor is very low in KGN cells, FSK, as a substitute for FSH, was utilized to activate FSH receptor in GCs and assess the effect of let-7i on steroidogenesis (38). The culture medium was assayed immediately; The concentration of estradiol (E2) in the conditioned medium was determined by an ELISA kit (CSB-E05108h; CUSABIO), as per the manufacturer's instructions. The assay was validated by the parallelism between the pooled and serial-diluted samples and the standard curve.

Dual-luciferase reporter assay

The luciferase reporter plasmids contain either wildtype 3'UTR segment of IMP2 (55335-1; GeneChem) or mutant 3'UTR segment of IMP2 (3'UTR-M, 55336-1; GeneChem). KGN cells grown in 24-well plates were co-transfected with 0.1 μg of the report plasmid and 0.02 μg of the Renilla luciferase plasmid, as well as 0.4 μg hsa-let-7i plasmid (55333-2; GeneChem) or miRNA empty vector plasmid (miRNA-NC) using X-tremegene HP (06366236001, Roche, Germany) transfection reagent. 48 h after transfection, the firefly and Renilla luciferase activities in the cell lysates were detected with the Dual-Luciferase Reporter Assay System (Promega) according to the manufacturer's instructions.

Statistical analysis

All data were analyzed by SPSS version 23.0 (IBM, Armonk, NY, USA) and GraphPad Prism version 7 (GraphPad, La Jolla, USA). The Shapiro-Wilk's test was used to assess whether the data had a Gaussian distribution. Comparisons between two groups were performed with Student's t test for quantitative data with a Gaussian distribution, or Mann–Whitney U-test for data with a non-Gaussian distribution. For data with more than two groups were analyzed by one-way analysis of variance (ANOVA) or the Kruskal-Wallis test. Correlation between let-7i expression and IMP2 expression groups was analyzed by Pearson's rank correlation test. QRT-PCR data were analyzed according to $2-\Delta\Delta Ct$ method. Data are shown as the mean ± standard deviation (SD) from at least three independent experiments. A P value of <0.05 was considered statistically significant. $^{*}P < 0.05$, $^{**}P < 0.01$, $^{***}P < 0.001$.

Results

In PCOS GCs, let-7i is down-regulated and IMP2 is up-regulated

To determine if the expression of let-7i is altered in GCs of PCOS patients compared to that of non-PCOS patients, a qRT-PCR assay was used to measure the expression of let-7i in a total of twenty-four GCs

samples from eleven PCOS patients and thirteen controls. Let-7i expression was lower in PCOS GCs than that in non-PCOS GCs (p□0.01; **Fig. 1A**). We also analyzed the potential targets of let-7i using bioinformatics analysis and evaluated the binding site strength of targets. On the basis of the result performed by bioinformatics analysis, we analyzed the relative mRNA expression of IMP1, IMP2 and IMP3 in human GCs. It was observed that the expression of IMP2 mRNA in GCs was significantly increased in PCOS patients compared to that in controls (p□0.01; **Fig. 1C**). However, no significant differences compared to the control group were observed in the expression of IMP1 mRNA (**Fig. 1B**) or in the expression of IMP3 mRNA (**Fig. 1D**). Western blot analysis showed that the expression of IMP2 protein in PCOS GCs was higher than that in controls, and the tendency of change was coincident with the increased expression of IMP2 mRNA (p□0.05; **Fig. 1E**). Moreover, we analyzed the association between the expression of let-7i and the expression IMP2 mRNA in GCs. As shown in **Fig. 1F**, there was a negative correlation between the expression of let-7i and the expression IMP2 mRNA (R=-0.6452, P□0.01).

Let-7i overexpression inhibits KGN cells proliferation and arrests the cell cycle

On the basis of the above results, we determined the effect of let-7i overexpression on KGN cells by using a transiently transfected let-7i mimics (150 nM). Known from qRT-PCR assay, the expression of let-7i in KGN cells was effectively overexpressed by let-7i mimics (p□0.001; **Fig. 2A**). Next, we used the EdU assay to determine whether let-7i in involved in cell proliferation. The EdU assay showed less EdU-positive cells in let-7i mimics group (p□0.05; **Fig. 2B** and **C**). To explore the potential mechanisms of let-7i overexpression on GCs proliferation, we performed cell cycle analysis by PI staining and flow cytometry. We found that the percentage of S-phase cells was decreased (p□0.05) and the percentage of G1-phase cells (p□0.01) was increased in let-7i-overexpressed cells at 48 h post-transfection compared with control group (**Fig. 2D** and **E**). These results verified that let-7i markedly suppressed GC proliferation by inducing G1 cell cycle arrest. The CCK-8 assay revealed the overexpression of let-7i reduced the viability of KGN cells at 48 h and 72 h post-transfection of let-7i mimics (p□0.01; **Fig. 2F**). The KGN cells were becoming less viable in let-7i mimics group in part by inhibiting cell proliferation. The decrease in cell viability might be caused by either reduced proliferation or excessive apoptosis. Thus, we further explored the role of overexpressed let-7i in apoptosis of GCs. However, no significant differences compared to the control group were observed in the rate of apoptotic cells (**Supplementary Fig.1**). These results indicated that the overexpression of let-7i inhibited the proliferation of GCs in part by arresting cell cycle rather than by inducing apoptosis.

Inhibition of let-7i promotes KGN proliferation

To further confirm the role of let-7i in GCs proliferation, loss-of-function experiment was performed in KGN cells. As shown in **Fig. 3A**, the expression of let-7i in KGN cells was down-regulated by transient transfection of let-7i inhibitors (150 nM) (p□0.001). The EdU assay showed more EdU-positive cells in let-7i inhibitors group (p□0.05; **Fig. 3B** and **C**). PI staining and flow cytometry revealed that when let-7i was inhibited, the percentage of S- and G2-phase cells was increased (p□0.05) and the percentage of G1-phase cells was decreased (p□0.05; **Fig. 3D** and **E**). CCK-8 assay showed that inhibition of let-7i increased

viability of KGN cells at 48 h and 72 h post-transfection of let-7i inhibitors (p□0.05; **Fig. 3F**). These data suggested that loss of let-7i mediated the promotion of GCs proliferation.

Overexpression of let-7i inhibits aromatase expression and decreases E2 production

Testosterone (T), as a substrate for aromatase, is converted to E2 under the action of aromatase in GCs. Since the expression level of functional FSH receptor is very low in KGN cells, FSK, as a substitute for FSH, was utilized to activate FSH receptor in GCs and assess the effect of let-7i on steroidogenesis. In the medium in the absence of T (100 nM) and FSK (1 μM), E2 content was low (□100 pg/mL; **Fig. 4A**), and the concentrations of E2 after let-7i mimics treatment showed no difference compared with the control group (**Fig. 4B**). After the addition of T, the E2 concentrations increased significantly (p□0.01), especially in the presence of T and FSK (p□0.001; **Fig. 4A**). To investigate the role of let-7i in steroidogenesis, we treated KGN cells for 24 h with T (100 nM) and FSK (1 μM) at 48 h post-transfection of let-7i mimics or inhibitors, and then determined the relative aromatase mRNA (*CYP19A1*) levels and relative protein expression of aromatase. Compared with the control group, E2 concentration was significantly decreased at 48 h post-transfection of let-7i mimics (p□0.05; **Fig. 4C**). Let-7i mimics significantly decreased the CYP19A1 mRNA expression in KGN cells (p□0.05; **Fig. 4E**), as well as the protein expression of aromatase (p□0.05; **Fig. 4G** and **H**). Let-7i inhibitors had the opposite effect, increasing the concentration of E2 (p□0.05; **Fig. 4D**) and CYP19A1 mRNA expression (p□0.05; **Fig. 4F**). These results verified that let-7i inhibited aromatase expression and decreased E2 production.

IMP2 is a target of let-7i

As mentioned above, we used bioinformatics analysis and qRT-PCR investigating the molecular mechanism of let-7i. We found that IMP1, IMP2 and IMP3 may be targets of let-7i. To verify the regulation of let-7i on target genes, qRT-PCR was performed and indicated that IMP2 mRNA expression was significantly decreased in KGN cells treated with let-7i mimics (p□0.05), while no significant differences in IMP1 and IMP3 mRNA (**Supplementary Fig. 2**). Hence, our subsequent experiments were focused on whether IMP2 was the target gene of let-7i in GCs. Our results showed that let-7i mimics (150 nM) decreased IMP2 mRNA levels (p□0.001; **Fig. 5A**), while let-7i inhibitors (150 nM) increased IMP2 mRNA levels (p□0.05; **Fig. 5B**). Let-7i mimics (50 nM – 200 nM) and let-7i inhibitors (100 nM – 250 nM) inhibited and promoted the protein expression of IMP2, respectively, with the most significant effect at 150 nM (**Fig. 5C** and **D**). To further confirm IMP2 was a direct target of let-7i, we analyzed the complementary sequence of let-7i in IMP2 3'UTR using the bioinformatics analysis and determined the mutant sites in IMP2 3'UTR (**Fig. 5E**). The results of dual-luciferase reporter assay revealed that overexpression of let-7i attenuated the luciferase activity of wild-type construct of IMP2 3'UTR compared with miRNA-control (miRNA-NC), whereas mutant 3'UTR (3'UTR-M) showed no response to let-7i (**Fig. 5F**). Taken together, these data demonstrated that IMP2 is a direct downstream target of let-7i.

IMP2 mediates the effects of let-7i on GCs

Rescue experiments were performed to confirm whether let-7i executed its functional effects by suppressing IMP2. Let-7i mimics-transfected KGN cells were infected with lentiviruses expressing IMP2 (lenti-IMP2). Lenti-IMP2 upregulated the IMP2 mRNA (p□0.01) and protein expression (p□0.05) in KGN cells (**Fig. 6A** and **B**). After the restoration of IMP2 expression, the protein expression of aromatase was up-regulated (p□0.01; **Fig. 6B**). Reintroduction of IMP2 reversed the effect of let-7i mimics on KGN cells. Cell cycle assay confirmed that overexpression of IMP2 significantly increased the cells in S- and G2-phase, and decreased the cells in the G1 phase (p□0.001; **Fig. 6C**). The EdU assay and CCK-8 showed that overexpression of IMP2 abolished the let-7i-mediated inhibition effects on proliferation in KGN cells (**Fig. 6F** and **G**). Moreover, we used three small interfering RNAs (si-IMP2-1, si-IMP2-2, and si-IMP2-3) to silence IMP2 expression and found that only the si-IMP2-3 could effectively silence IMP2 expression (**Fig. 7A** and **B**). Silencing of IMP2 expression by si-IMP2 (si-IMP2-3) reversed the promoting function of let-7i loss on KGN cells proliferation. Knockdown of IMP2 decreased cell viability at 48 h (p□0.05) and 72 h (p□0.01) post-transfection of si-IMP2 (**Fig. 7C**), led to a transition arrest of G1 phase to S phase (p□0.01; **Fig. 7D**), and inhibited cell proliferation (p□0.001; **Fig. 7E**). Also, knockdown of IMP2 inhibited E2 production (p□0.05; **Fig.7F**), and abolished the effect of let-7i inhibitors on the steroidogenesis of GCs (p□0.05; **Fig. 7G**). These results indicated that IMP2 acted as a functional downstream target of let-7i in KGN cells.

Discussion

In the family of let-7, let-7i has a critical role in folliculogenesis with the highest level of expression in oocyte and GCs from different staged-follicles (22-24). Our present study was the first to obtain the differential expression of let-7i in GCs from women with PCOS and those without. Results showed that the expression of let-7i was significantly decreased in PCOS GCs compared with that in controls. A recent study reported that the expression of let-7i was increased in the serum from PCOS patients compared to serum samples in control women. There is a possible difference between data from Butler et al. and our studies, which probably because we tested ovarian GCs samples rather than serum samples. Therefore, the issues relative to samples will be further analyzed for PCOS in our future studies for let-7i.

Following the identification of potential prognostic value of let-7i in PCOS GCs, its biological role was analyzed in GCs. We used an immortalized human GC cell line KGN as the difficulties in obtaining adequate quantity of human GCs and in maintaining primary cultures. Many studies have reported the excessive proliferation of granulosa cells in PCOS patients, which may be related to the over-recruitment of follicles. An in-depth study of the molecular mechanism of granulosa cell growth and differentiation is of great help to the etiology of PCOS. We explored whether let-7i regulates KGN cells growth. Results indicated that overexpression of let-7i inhibited KGN cells proliferation, in part by arresting cell cycle, not by inducing cell apoptosis. Knockdown of let-7i promoted proliferation of KGN cells. Therefore, low levels of let-7i in GCs might account for the overgrowth of GCs in PCOS.

In addition to abnormal granulosa cell proliferation, PCOS patients often have abnormal steroid hormone metabolism. Multiple miRNAs have been identified the association with hormone metabolism disorder in PCOS. Upregulation of miR-320 suppresses the E2 production via SF-1, which may account for the

hyperandrogenism in PCOS (39). MiR-186 and miR-135a promote GCs proliferation by targeting ESR2 and could be regulated by E2 (10). It has been reported that in prostate cancer cells, androgen can inhibit the expression of let-7c through androgen receptor (40). Our study found that let-7i suppressed the aromatase mRNA (CYP19A1) and aromatase protein expression, and decreased the E2 production. Hyperandrogenemia is one of the main characteristics of PCOS patients. As an important androgen metabolizing enzyme, aromatase in GCs is involved in the encoding of CYP19A1 gene and can convert androgens to estrogen. There is still much debate about the expression and activity of aromatase in PCOS patients. Studies have reported that down-regulated CYP19A1 in PCOS patients leads to androgen accumulation as the pathogenic cause. Some contrary views claimed that aromatase activity and E2 production were increased in PCOS patients, which probably led to follicular development arrest at the stage of dominant follicle selection. Moreover, it has been reported that chronically elevated circulatory E2 likely plays a role in the pathogenesis of PCOS. In this study, we found that let-7i was down-regulated in the PCOS patients, but the characteristics of PCOS patients didn't show significant elevated circulatory E2. On the one hand, because the source of estrogen is extensive, E2 production is regulated by a variety of complex factors, not only affected by the gonad. Also, patients receiving IVF-ET/ICSI were included in our collection. Hormone levels would be affected by ovulation induction regimen, so we need to improve the methods of purification and separation of granulose cells to reduce these effects. On the other hand, perhaps due to the insufficient sample size we collected, we need to further expand the sample size for in-depth study.

Next, the underlying molecular mechanisms were to realize how let-7i mediated a suppressive role in proliferation of KGN cells. Bioinformatics analysis predicted 116 potential targets of let-7i overlapping in all three databases. According to the evaluation of binding site strength, we found that three paralogs in insulin-like growth factor 2 mRNA binding protein (IMP) family, IMP1, IMP2, and IMP3, were all unverified genes with high predicted binding-scores. IMPs are highly conserved oncofetal RNA-binding proteins that regulate RNA localization, stability and translation, and they share highly identical structural features with two RNA recognition motifs in N-terminal and four heterogeneous nuclear ribonucleoprotein K-homologous domains (41). These three paralogs (IMP1-3) have been identified that are expressed in ovary (31) and embryo (30). IMP2 expression is more widely and persistently expressed in ovarian GCs and oocyte than the expression of IMP1 and IMP3. IMP2 has the association with metabolic syndrome (42), such as insulin resistance (43) and obesity (44), contributing to increased risks of type 2 diabetes (45). Intriguingly, a recent study reported that the expression of IMP2 was increased in PCOS GCs and overexpression of IMP2 promoted GCs proliferation (31). IMP2 can be regulated by miRNAs (miR-216b or miR-596, for instance) and affects various cellular physiological process (46, 47). Here our study confirmed that IMP2 was a direct functional target of let-7i in KGN cells. At first, we measured the expression of IMP1-3 in GCs of patients and controls, as IMPs have similar structure in terms of domain order and spacing. We confirmed that the expression of IMP2 was increased in PCOS GCs compared with that in controls and the expression levels of let-7i and IMP2 were inversely correlated in human GCs. Next, our data indicated that let-7i can inhibit the levels of both mRNA and protein of IMP2 in KGN cells. Luciferase reporter gene assay demonstrated that overexpression of let-7i significantly reduced the

activity of a luciferase reporter containing the 3'UTR sequence of IMP2. To verify whether IMP2 mediated the effects of let-7i in KGN cells, rescue experiments were performed to examine the roles of IMP2 in proliferation and cell cycle. Our data indicated that reintroduction of IMP2 expression antagonized the inhibitory effects of let-7i on KGN cell proliferation and aromatase expression, and knockdown of IMP2 reversed the promoted roles of let-7i in cell proliferation and E2 production, suggesting that IMP2 is a predominant functional target of let-7i in these processes. Since our functional experiments were performed in the KGN cell line, further validation would need to be extend them to human primary GCs and animal models. Also, it is interesting to identify the key downstream signaling pathways of IMP2 in GCs proliferation and E2 biosynthesis. A study has demonstrated that IMP2 binds the 3'UTR of CCND2 and SERBP1 mRNAs, increases the expression of these protein and thus promotes the proliferation of GCs. In future, we will perform experiments on animals to investigate whether the effects of let-7i/IMP2 on GCs proliferation and E2 production are related to the causes of PCOS or are a consequence of the progression of PCOS.

In addition to abnormal GCs proliferation and hormonal metabolism disorders in PCOS, A growing number of studies have shown that PCOS is associated with markers of inflammation and insulin sensitivity. The levels of interleukin-6 (IL-6), interleukin-8 (IL-8), and interleukin-1β (IL-1β) were elevated in follicular fluid or serum of PCOS patients compared with that of non-PCOS patients (48-50). Let-7 has been reported as an immuno-repressor involved in the inflammatory process (51). We found that let-7i significantly inhibited the expression of IL-6, IL-8, and IL-1β mRNA (**Supplementary Fig. 3**), suggesting the its potential as a therapeutic target for PCOS. It will be interesting to explore the relationship between the let-7i-IMP2 pathway and inflammatory markers in PCOS.

In conclusion, to our knowledge, we presented the first evidence that let-7i expression was decreased in PCOS GCs and let-7i inhibited GCs proliferation, aromatase expression and E2 production by directly targeting IMP2. Understanding the roles of let-7i involved in GCs function will help us to identify its potential prognostic and therapeutic values in PCOS.

Abbreviations

PCOS, Polycystic ovary syndrome; GCs, granulosa cells; miRNA, microRNA; let-7, lethal-7; IMP, insulin-like growth factor 2 mRNA binding protein; IMP2, insulin-like growth factor 2 mRNA binding protein 2; IVF-ET/ICSI, in vitro fertilization-embryo transfer/intracytoplasmic sperm injection; BMI, body mass index; E2, estradiol; P4, progesterone; FSH, follicle-stimulating hormone; LH, luteinizing hormone; T, testosterone; PRL, prolactin; TSH, thyroid stimulating hormone; AMH, anti-Mullerian hormone; lenti-IMP2, lentiviruses expressing IMP2; lenti-ctrl, the control group lentiviruses; siRNA, small interfering RNA; si-IMP2, small interfering RNA targeting IMP2; si-ctrl, siRNA controls; si-1, si-IMP2-1; si-2, si-IMP-2; si-3, si-IMP2-3; mi-ctrl, mimics-negative control; in-ctrl, inhibitors-negative control; qRT-PCR, quantitative real-time polymerase chain reaction; EdU, 5-ethynyl-2'-deoxyuridine; PI, propidium iodide; cck-8, cell counting kit-8; 3'UTR, 3'-untranslated regions; 3'UTR-M, mutant 3'UTR segment of IMP2; miRNA-NC, miRNA negative control plasmid; IL-6, interleukin-6; IL-8, interleukin-8; IL-1β, interleukin-1β.

Declarations

Ethics approval and consent to participate

The Human Research Ethics Committee of the Obstetrics and Gynecology Hospital of Fudan University approved the study.

Consent for publication

Not applicable.

Availability of data and materials

All data generated or analyzed during this study are included in this published article.

Competing interests

The authors declare that they have no completing interests.

Funding

This study was supported by the Natural Science Foundation of the Science and Technology Commission of Shanghai Municipality (grant No. 17ZR1403100 to Xue-Lian Li).

Authors' contributions

X. L. conceived and designed the study; M.D supervised this study; X. X. and L. C. performed the in vitro experiments; M. Y. performed the processing of clinical samples and H. S. contributed to data analysis; X. X. drafted the manuscript and L.C. reviewed the manuscript. X. L. provided funding, helped to review the manuscript and approved its final version.

Acknowledgements

We acknowledge the editors and reviewers for their insightful suggestions regarding this work.

References

1. Azziz R, Carmina E, Chen Z, et al. Polycystic ovary syndrome. Nature reviews Disease primers. 2016;2:16057. doi:10.1038/nrdp.2016.57.
2. Boyle JA, Teede HJ. PCOS: Refining diagnostic features in PCOS to optimize health outcomes. Nature reviews Endocrinology. 2016;12(11):630–1. doi:10.1038/nrendo.2016.157.
3. Azziz R. Polycystic Ovary Syndrome. Obstetrics gynecology. 2018;132(2):321–36. doi:10.1097/aog.0000000000002698.

4. Escobar-Morreale HF. Polycystic ovary syndrome: definition, aetiology, diagnosis and treatment. Nature reviews Endocrinology. 2018;14(5):270–84. doi:10.1038/nrendo.2018.24.
5. Das M, Djahanbakhch O, Hacihanefioglu B, et al. Granulosa cell survival and proliferation are altered in polycystic ovary syndrome. J Clin Endocrinol Metab. 2008;93(3):881–7. doi:10.1210/jc.2007-1650.
6. Stubbs SA, Stark J, Dilworth SM, Franks S, Hardy K. Abnormal preantral folliculogenesis in polycystic ovaries is associated with increased granulosa cell division. J Clin Endocrinol Metab. 2007;92(11):4418–26. doi:10.1210/jc.2007-0729.
7. Dumesic DA, Meldrum DR, Katz-Jaffe MG, Krisher RL, Schoolcraft WB. Oocyte environment: follicular fluid and cumulus cells are critical for oocyte health. Fertility sterility. 2015;103(2):303–16. doi:10.1016/j.fertnstert.2014.11.015.
8. Biase FH, Kimble KM. Functional signaling and gene regulatory networks between the oocyte and the surrounding cumulus cells. BMC Genomics. 2018;19(1):351. doi:10.1186/s12864-018-4738-2.
9. Kong F, Du C, Wang Y. MicroRNA-9 affects isolated ovarian granulosa cells proliferation and apoptosis via targeting vitamin D receptor. Molecular cellular endocrinology. 2019;486:18–24. doi:10.1016/j.mce.2019.02.012.
10. Song Y, Yu G, Xiang Y, Li Y, Wan L, Tan L. Altered miR-186 and miR-135a contribute to granulosa cell dysfunction by targeting ESR2: A possible role in polycystic ovary syndrome. Molecular cellular endocrinology. 2019;494:110478. doi:10.1016/j.mce.2019.110478.
11. Liu S, Zhang X, Shi C, et al. Altered microRNAs expression profiling in cumulus cells from patients with polycystic ovary syndrome. Journal of translational medicine. 2015;13:238. doi:10.1186/s12967-015-0605-y.
12. Xue Y, Lv J, Xu P, et al. Identification of microRNAs and genes associated with hyperandrogenism in the follicular fluid of women with polycystic ovary syndrome. Journal of cellular biochemistry. 2018;119(5):3913–21. doi:10.1002/jcb.26531.
13. Tu J, Cheung AH, Chan CL, Chan WY. The Role of microRNAs in Ovarian Granulosa Cells in Health and Disease. Front Endocrinol. 2019;10:174. doi:10.3389/fendo.2019.00174.
14. Lee H, Han S, Kwon CS, Lee D. Biogenesis and regulation of the let-7 miRNAs and their functional implications. Protein cell. 2016;7(2):100–13. doi:10.1007/s13238-015-0212-y.
15. Hossain MM, Sohel MM, Schellander K, Tesfaye D. Characterization and importance of microRNAs in mammalian gonadal functions. Cell tissue research. 2012;349(3):679–90. doi:10.1007/s00441-012-1469-6.
16. Zolbin MM, Mamillapalli R, Nematian SE, Goetz L, Taylor HS. Adipocyte alterations in endometriosis: reduced numbers of stem cells and microRNA induced alterations in adipocyte metabolic gene expression. Reproductive biology endocrinology: RB&E. 2019;17(1):36. doi:10.1186/s12958-019-0480-0.
17. McWhorter ES, West RC, Russ JE, Ali A, Winger QA, Bouma GJ. LIN28B regulates androgen receptor in human trophoblast cells through Let-7c. Mol Reprod Dev. 2019;86(9):1086–93.

doi:10.1002/mrd.23226.

18. Zhao Y, Deng C, Lu W, et al. let-7 microRNAs induce tamoxifen sensitivity by downregulation of estrogen receptor α signaling in breast cancer. Molecular medicine (Cambridge Mass). 2011;17:1233–41. doi:10.2119/molmed.2010.00225.
19. Jun-Hao ET, Gupta RR, Shyh-Chang N. Lin28 and let-7 in the Metabolic Physiology of Aging. Trends Endocrinol Metab. 2016;27(3):132–41. doi:10.1016/j.tem.2015.12.006.
20. Zhou J, Liu J, Pan Z, et al. The let-7g microRNA promotes follicular granulosa cell apoptosis by targeting transforming growth factor-β type 1 receptor. Molecular cellular endocrinology. 2015;409:103–12. doi:10.1016/j.mce.2015.03.012.
21. Otsuka M, Zheng M, Hayashi M, et al. Impaired microRNA processing causes corpus luteum insufficiency and infertility in mice. J Clin Investig. 2008;118(5):1944–54. doi:10.1172/jci33680.
22. Gilchrist GC, Tscherner A, Nalpathamkalam T, Merico D, LaMarre J. MicroRNA Expression during Bovine Oocyte Maturation and Fertilization. Int J Mol Sci. 2016;17(3):396. doi:10.3390/ijms17030396.
23. Cao R, Wu WJ, Zhou XL, Xiao P, Wang Y, Liu HL. Expression and preliminary functional profiling of the let-7 family during porcine ovary follicle atresia. Mol Cells. 2015;38(4):304–11. doi:10.14348/molcells.2015.2122.
24. Wong QW, Sun MA, Lau SW, et al. Identification and characterization of a specific 13-miRNA expression signature during follicle activation in the zebrafish ovary. Biol Reprod. 2018;98(1):42–53. doi:10.1093/biolre/iox160.
25. Butler AE, Ramachandran V, Sathyapalan T, et al. microRNA Expression in Women With and Without Polycystic Ovarian Syndrome Matched for Body Mass Index. Front Endocrinol. 2020;11:206. doi:10.3389/fendo.2020.00206.
26. Ding CF, Chen WQ, Zhu YT, Bo YL, Hu HM, Zheng RH. Circulating microRNAs in patients with polycystic ovary syndrome. Hum Fertil (Cambridge England). 2015;18(1):22–9. doi:10.3109/14647273.2014.956811.
27. Müller-McNicoll M, Neugebauer KM. How cells get the message: dynamic assembly and function of mRNA-protein complexes. Nature reviews Genetics. 2013;14(4):275–87. doi:10.1038/nrg3434.
28. Liu HB, Muhammad T, Guo Y, et al. RNA-Binding Protein IGF2BP2/IMP2 is a Critical Maternal Activator in Early Zygotic Genome Activation. *Advanced science (Weinheim, Baden-Wurttemberg, Germany)*. 2019;6(15):1900295. doi:10.1002/advs.201900295.
29. Drouilhet L, Mansanet C, Sarry J, et al. The highly prolific phenotype of Lacaune sheep is associated with an ectopic expression of the B4GALNT2 gene within the ovary. PLoS Genet. 2013;9(9):e1003809. doi:10.1371/journal.pgen.1003809.
30. Haouzi D, Dechaud H, Assou S, Monzo C, de Vos J, Hamamah S. Transcriptome analysis reveals dialogues between human trophectoderm and endometrial cells during the implantation period. Human reproduction (Oxford England). 2011;26(6):1440–9. doi:10.1093/humrep/der075.

31. Li M, Zhao H, Zhao SG, et al. The HMGA2-IMP2 Pathway Promotes Granulosa Cell Proliferation in Polycystic Ovary Syndrome. J Clin Endocrinol Metab. 2019;104(4):1049–59. doi:10.1210/jc.2018-00544.
32. Revised. 2003 consensus on diagnostic criteria and long-term health risks related to polycystic ovary syndrome. *Fertility and sterility*. 2004;81(1):19–25. doi:10.1016/j.fertnstert.2003.10.004.
33. He T, Sun Y, Zhang Y, et al. MicroRNA-200b and microRNA-200c are up-regulated in PCOS granulosa cell and inhibit KGN cell proliferation via targeting PTEN. Reproductive biology endocrinology: RB&E. 2019;17(1):68. doi:10.1186/s12958-019-0505-8.
34. Ye H, Liu XJ, Hui Y, Liang YH, Li CH, Wan Q. via PtenDownregulation of MicroRNA-222 Reduces Insulin Resistance in Rats with PCOS by Inhibiting Activation of the MAPK/ERK Pathway. Molecular therapy Nucleic acids. 2020;22:733–41. doi:10.1016/j.omtn.2020.07.014.
35. Xu X, Chen X, Zhang X, et al. Impaired telomere length and telomerase activity in peripheral blood leukocytes and granulosa cells in patients with biochemical primary ovarian insufficiency. Human reproduction (Oxford England). 2017;32(1):201–7. doi:10.1093/humrep/dew283.
36. Nishi Y, Yanase T, Mu Y, et al. Establishment and characterization of a steroidogenic human granulosa-like tumor cell line, KGN, that expresses functional follicle-stimulating hormone receptor. Endocrinology. 2001;142(1):437–45. doi:10.1210/endo.142.1.7862.
37. Li Y, Liu YD, Zhou XY, et al. MiR-29a regulates the proliferation, aromatase expression, and estradiol biosynthesis of human granulosa cells in polycystic ovary syndrome. Molecular cellular endocrinology. 2019;498:110540. doi:10.1016/j.mce.2019.110540.
38. Nagao S, Iwata N, Soejima Y, et al. Interaction of ovarian steroidogenesis and clock gene expression modulated by bone morphogenetic protein-7 in human granulosa cells. Endocrine journal. 2019;66(2):157–64. doi:10.1507/endocrj.EJ18-0423.
39. Yin M, Wang X, Yao G, et al. Transactivation of micrornA-320 by microRNA-383 regulates granulosa cell functions by targeting E2F1 and SF-1 proteins. J Biol Chem. 2014;289(26):18239–57. doi:10.1074/jbc.M113.546044.
40. Sun D, Layer R, Mueller AC, et al. Regulation of several androgen-induced genes through the repression of the miR-99a/let-7c/miR-125b-2 miRNA cluster in prostate cancer cells. Oncogene. 2014;33(11):1448–57. doi:10.1038/onc.2013.77.
41. Bell JL, Wächter K, Mühleck B, et al. Insulin-like growth factor 2 mRNA-binding proteins (IGF2BPs): post-transcriptional drivers of cancer progression? Cell Mol Life Sci. 2013;70(15):2657–75. doi:10.1007/s00018-012-1186-z.
42. Zhang Y, Kent JW, Olivier M, et al. QTL-based association analyses reveal novel genes influencing pleiotropy of metabolic syndrome (MetS). Obesity (Silver Spring Md). 2013;21(10):2099–111. doi:10.1002/oby.20324.
43. Vangipurapu J, Stančáková A, Pihlajamäki J, et al. Association of indices of liver and adipocyte insulin resistance with 19 confirmed susceptibility loci for type 2 diabetes in 6,733 non-diabetic Finnish men. Diabetologia. 2011;54(3):563–71. doi:10.1007/s00125-010-1977-4.

44. Dai N, Zhao L, Wrighting D, et al. IGF2BP2/IMP2-Deficient mice resist obesity through enhanced translation of Ucp1 mRNA and Other mRNAs encoding mitochondrial proteins. Cell Metabol. 2015;21(4):609–21. doi:10.1016/j.cmet.2015.03.006.
45. Huang Q, Yin JY, Dai XP, et al. IGF2BP2 variations influence repaglinide response and risk of type 2 diabetes in Chinese population. Acta pharmacologica Sinica. 2010;31(6):709–17. doi:10.1038/aps.2010.47.
46. Liu FY, Zhou SJ, Deng YL, et al. MiR-216b is involved in pathogenesis and progression of hepatocellular carcinoma through HBx-miR-216b-IGF2BP2 signaling pathway. Cell death disease. 2015;6:e1670. doi:10.1038/cddis.2015.46.
47. Fen H, Hongmin Z, Wei W, et al. RHPN1-AS1 Drives the Progression of Hepatocellular Carcinoma via Regulating miR-596/IGF2BP2 Axis. Curr Pharm Design. 2020;25(43):4630–40. doi:10.2174/1381612825666191105104549.
48. Cirillo F, Catellani C, Lazzeroni P, et al. MiRNAs Regulating Insulin Sensitivity Are Dysregulated in Polycystic Ovary Syndrome (PCOS) Ovaries and Are Associated With Markers of Inflammation and Insulin Sensitivity. Front Endocrinol. 2019;10:879. doi:10.3389/fendo.2019.00879.
49. Zuo T, Zhu M, Xu W, Wang Z, Song H. Iridoids with Genipin Stem Nucleus Inhibit Lipopolysaccharide-Induced Inflammation and Oxidative Stress by Blocking the NF-κB Pathway in Polycystic Ovary Syndrome. Cellular physiology biochemistry: international journal of experimental cellular physiology biochemistry pharmacology. 2017;43(5):1855–65. doi:10.1159/000484074.
50. Vgontzas AN, Trakada G, Bixler EO, et al. Plasma interleukin 6 levels are elevated in polycystic ovary syndrome independently of obesity or sleep apnea. Metab Clin Exp. 2006;55(8):1076–82. doi:10.1016/j.metabol.2006.04.002.
51. Jiang S. Recent findings regarding let-7 in immunity. Cancer letters. 2018;434:130–1. doi:10.1016/j.canlet.2018.07.027.

Tables

Due to technical limitations, table 1 and 2 is only available as a download in the Supplemental Files section.

Figures

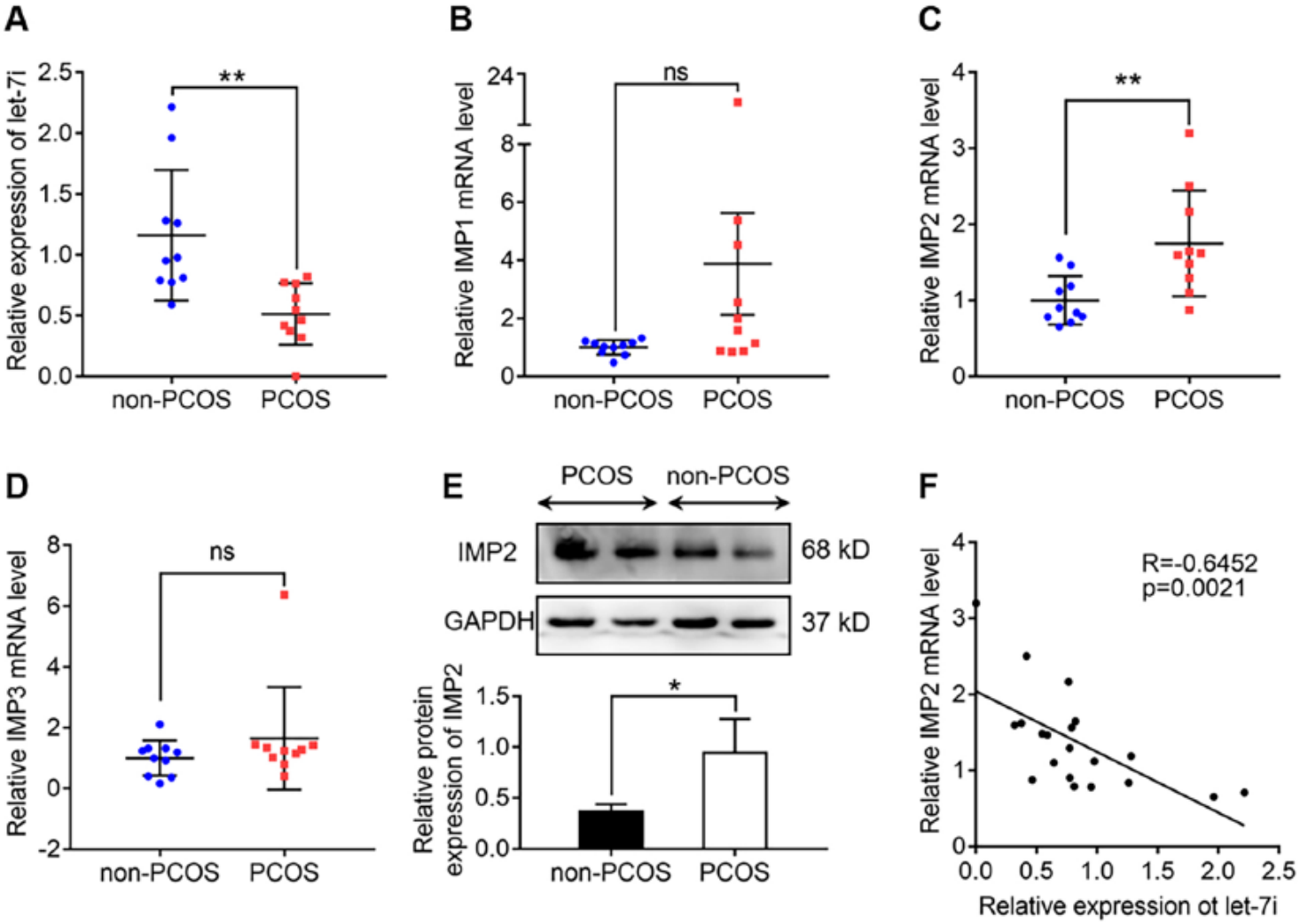

Figure 1

The expression of let-7i and IMP2 in human GCs. (A): The expression levels of let-7i in PCOS GCs were lower than those in non-PCOS GCs measured by qRT-PCR. (B-D): The expression levels of IMP1, IMP2 and IMP3 mRNA in PCOS GCs and those in non-PCOS GCs were measured by qRT-PCR. (E): Protein expression of IMP2 in PCOS GCs and those in non-PCOS GCs were measured using western blot. (F): The correlation between let-7i expression and IMP2 mRNA expression in patients. Data are shown as the mean ± SD. *P 0.05, **P < 0.01.

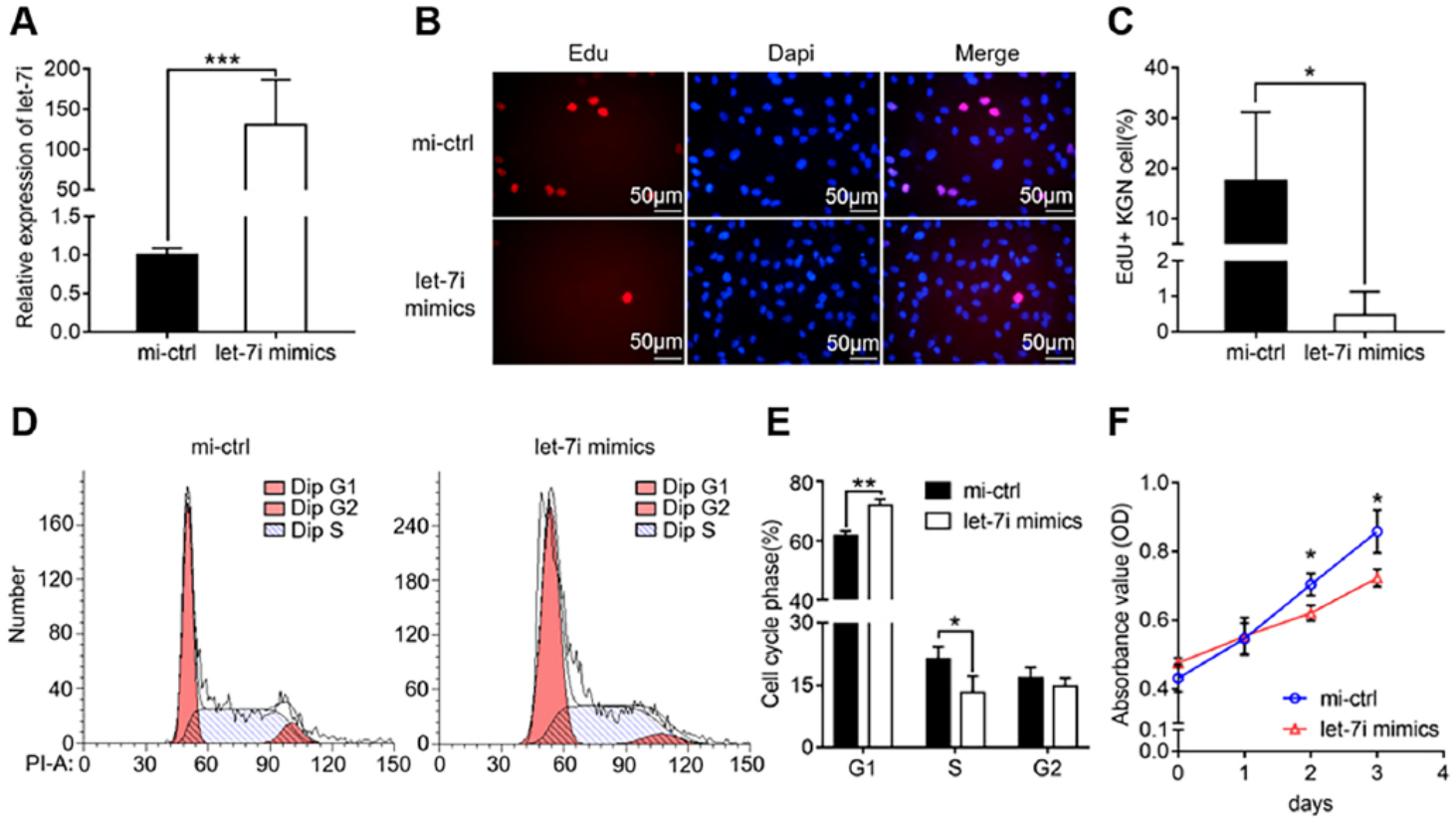

Figure 2

Overexpression of let-7i inhibited KGN cell proliferation and arrested the cell cycle. (A): The transfection efficiency was determined after incubation for 48 h with 150 nM let-7i mimics or mimics-negative control (mi-ctrl) in KGN cells, and the relative let-7i expression levels were measured by qRT-PCR. (B-C): EdU assay showed that percentage of proliferating cells (EdU/DAPI) was decreased in cells transfected with let-7i mimics compared with that in cells transfected with mi-ctrl. (D-E): PI staining and flow cytometry analysis displayed a significant increase of G1-phase cells and a decrease of S-phase cells in let-7i-overexpressed cells (at 48 h post-transfection). (F): The cell viability in cells transfected with let-7i mimics or mi-ctrl was measured using CCK-8 assays after 0-72 h. Data are shown as the mean ± SD from at least three independent experiments. *P < 0.05, **P < 0.01, ***P□0.001.

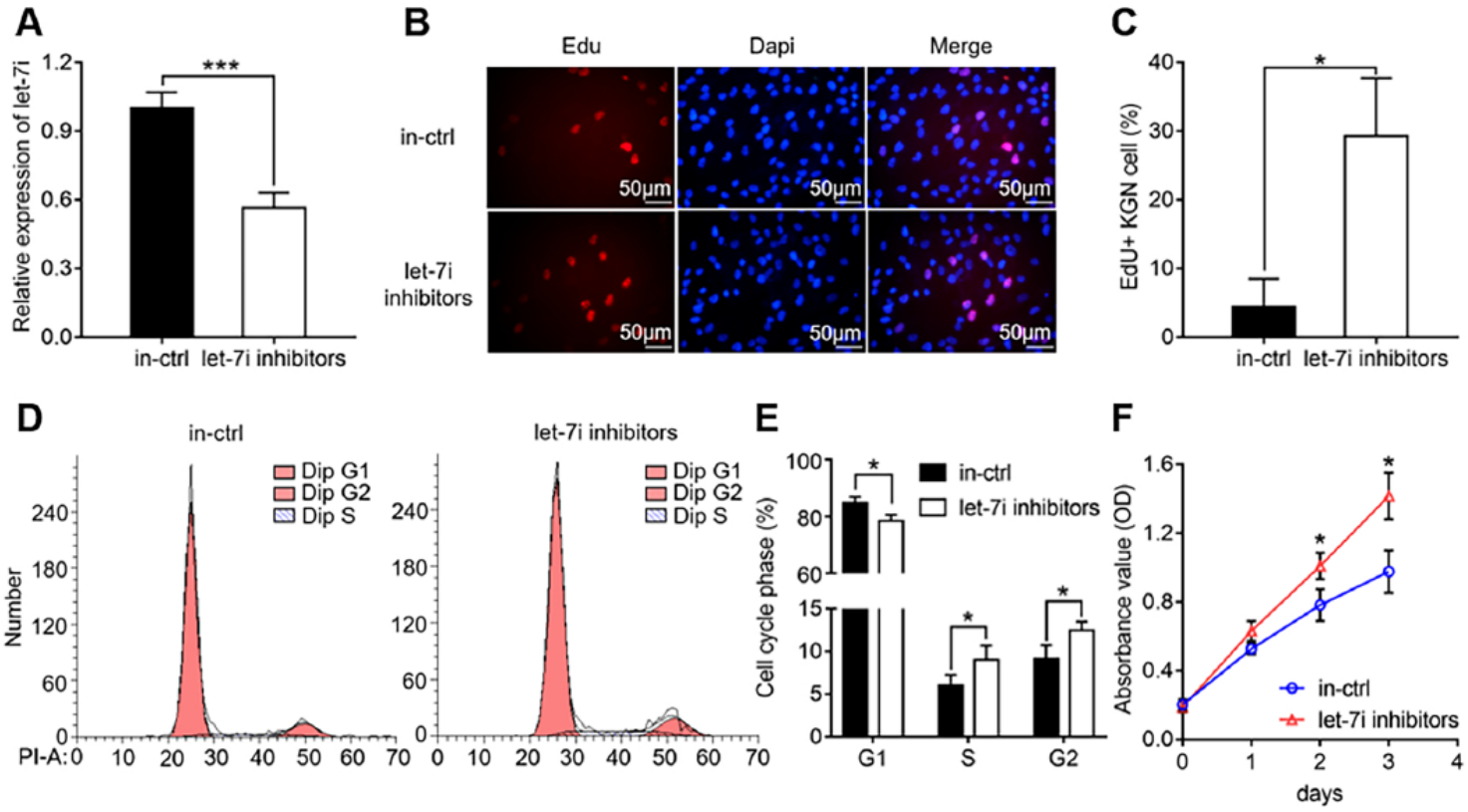

Figure 3

let-7i inhibitors promoted KGN cell proliferation. (A): The transfection efficiency was determined after incubation for 48 h with 150 nM let-7i inhibitors or inhibitors-negative control (in-ctrl) in KGN cells, and the relative let-7i expression levels were measured by qRT-PCR. (B-C): EdU assay showed that percentage of proliferating cells was increased in cells transfected with let-7i inhibitors compared to controls. (D-E): PI staining and flow cytometry analysis displayed a decreased proportion of G1-phase cells and an increased proportion of S- and G2-phase cells in let-7i inhibitors group (at 48 h post-transfection). (F): The cell viability in cells transfected with let-7i inhibitors or in-ctrl was measured using CCK-8 assays after 0-72 h. Data are shown as the mean ± SD from at least three independent experiments. *P < 0.05, **P < 0.01, ***P < 0.001.

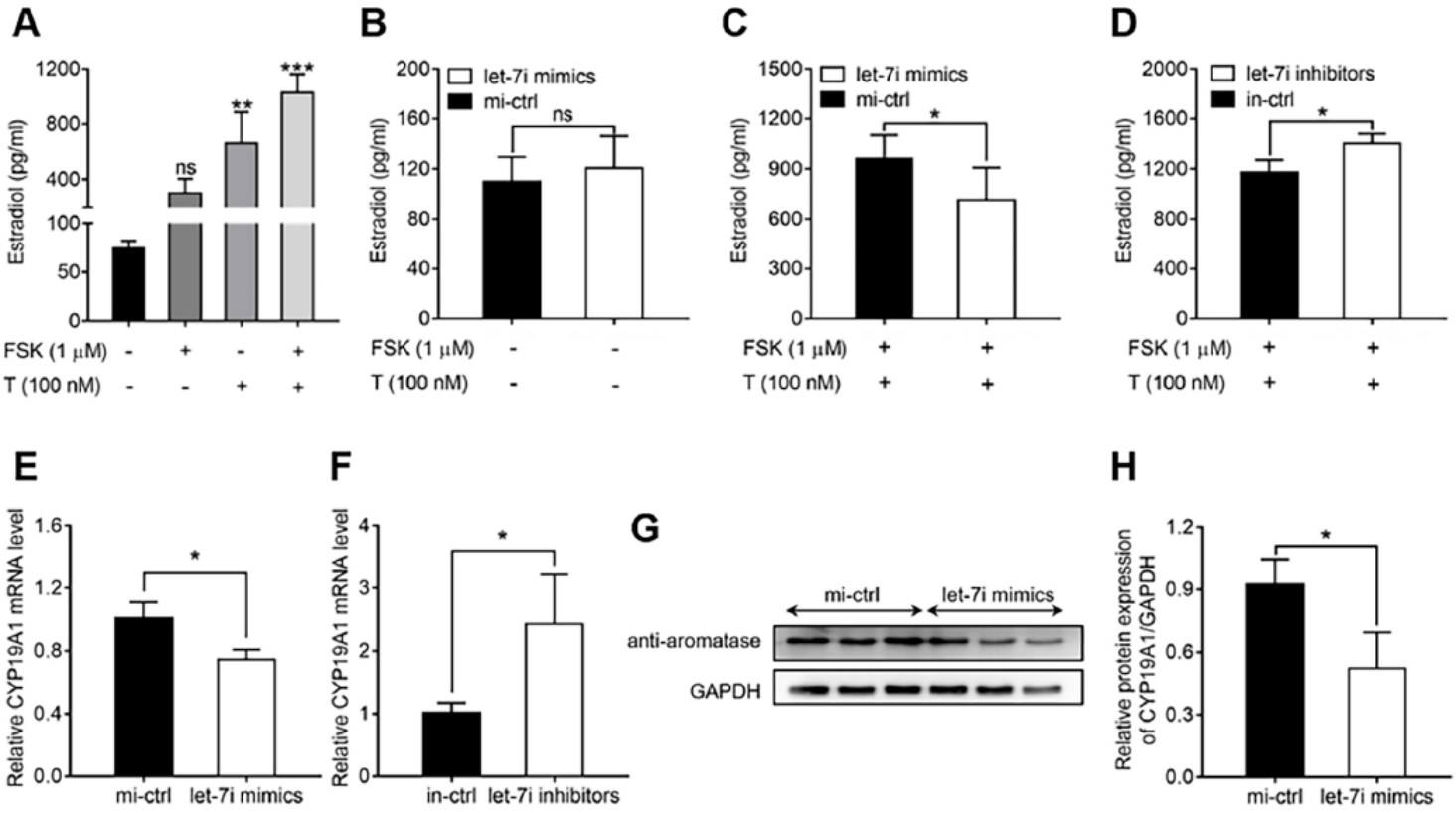

Figure 4

Effect of let-7i on aromatase expression and estradiol (E2) production. (A): The concentrations of E2 production in KGN cells was detected by an ELISA assay kit. (B-C): The effect of let-7i mimics on E2 production in the presence or absence of testosterone (T) and forskolin (FSK). (D): The effect of let-7i inhibitors on E2 production in the presence of T (100 nM) and FSK (1 μM). (E-F): Aromatase CYP19A1 mRNA levels were measured by qRT-PCR in KGN cells. (G-H): Aromatase protein levels were measured by western blot analysis in KGN cells. Data are shown as the mean ± SD from at least three independent experiments. *P < 0.05, **P < 0.01, ***P < 0.001.

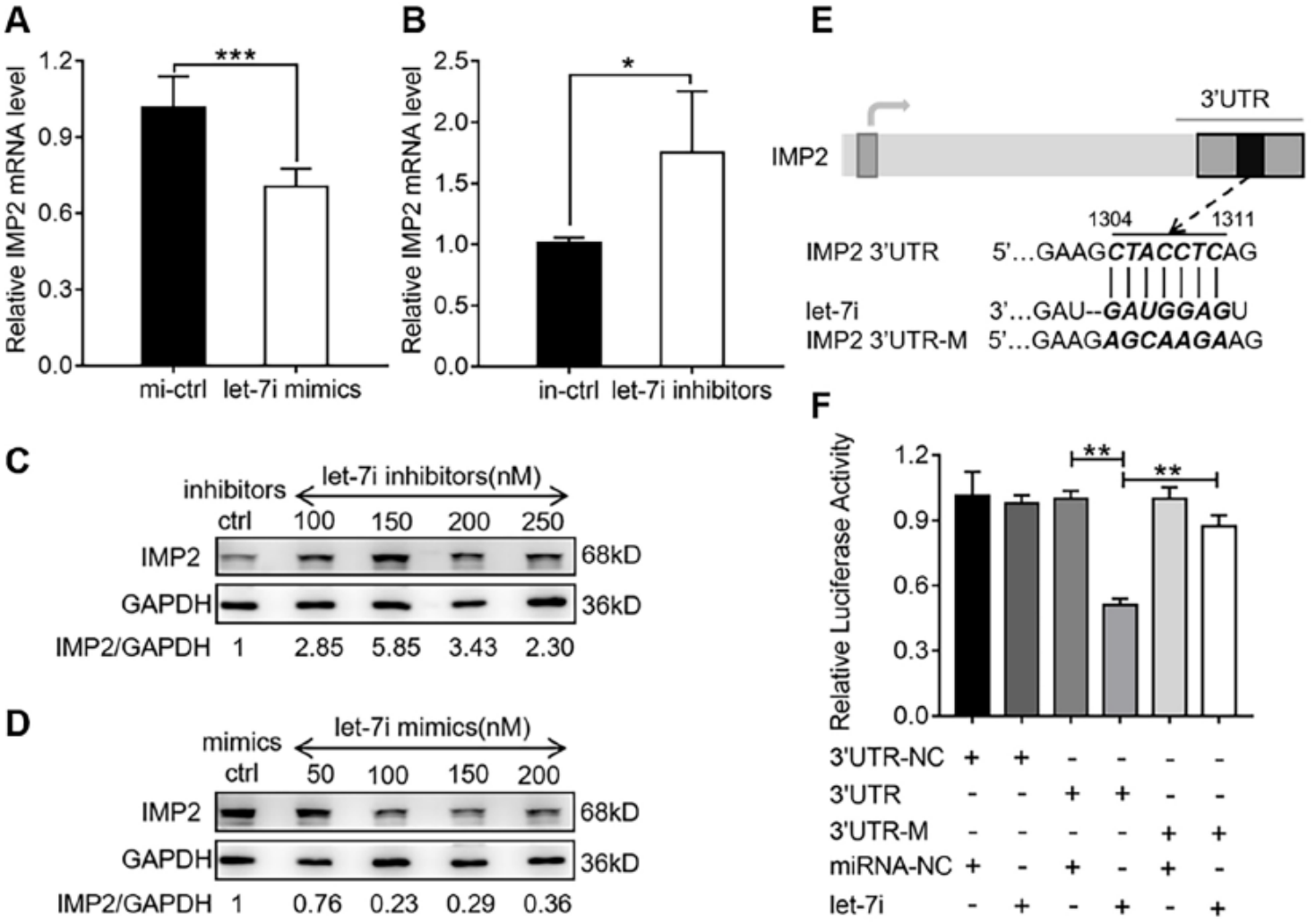

Figure 5

IMP2 is a direct target of let-7i. (A-B): The IMP2 mRNA levels in KGN cells transfected with 150 nM of let-7i mimics or let-7i inhibitors were measured by qRT-PCR. (C): Protein expression of IMP2 in KGN cells transfected with let-7i inhibitors and inhibitors-negative control (in-ctrl) was measured using western blot analysis. (D): Protein expression of IMP2 in cells transfected with let-7i mimics and mimics-negative control (mi-ctrl) was measured using western blot analysis. (E): Structure diagram showed the predicted binding sites and corresponding mutant sites of IMP2. (F): Dual-luciferase reporter gene assay verified the direct relationship of let-7i and IMP2. Data are shown as the mean ± SD from at least three independent experiments. *P < 0.05, **P < 0.01, ***P < 0.001.

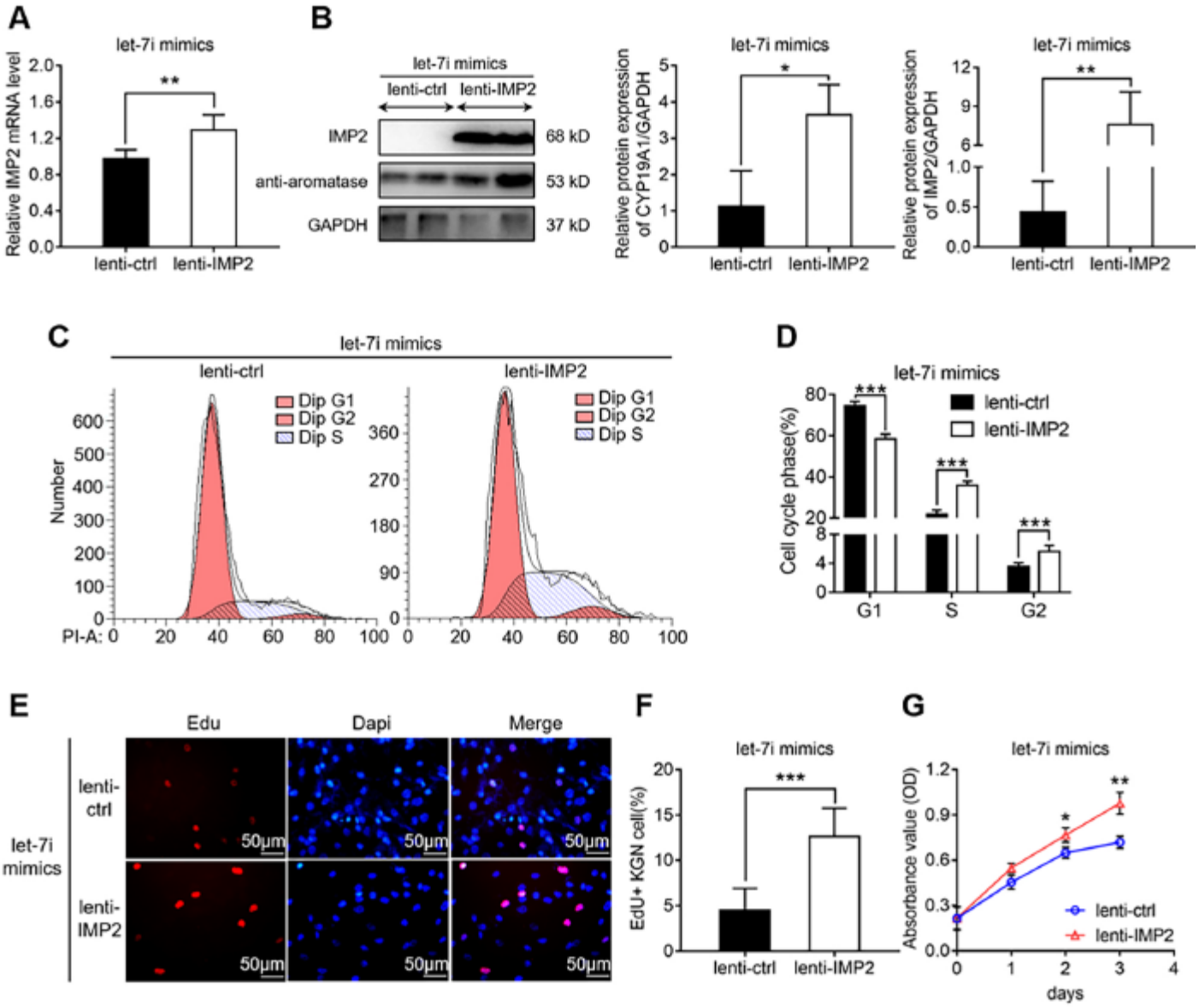

Figure 6

Modulation of IMP2 expression reverses let-7i-mediated cellular activities. (A): The IMP2 mRNA levels in let-7i mimics group transfected with lenti-IMP2 vector or the control vector (lenti-ctrl) were measured by qRT-PCR. (B): Western blot showed the protein expression of IMP2 and aromatase in let-7i mimics group transfected with lenti-IMP2 or lenti-ctrl. (C-D): Cell cycle in let-7i mimics group transfected with lenti-IMP2 or lenti-ctrl was measured by PI staining and flow cytometry analysis. (E-F): EdU assay showed the effects of lenti-IMP2 and lenti-ctrl on the proliferation of KGN cells in let-7i mimics group. (G): CCK-8 indicated that IMP2 restoration increased the cell viability of KGN cells. Data are shown as the mean ± SD from at least three independent experiments. *P < 0.05, **P < 0.01, ***P < 0.001.

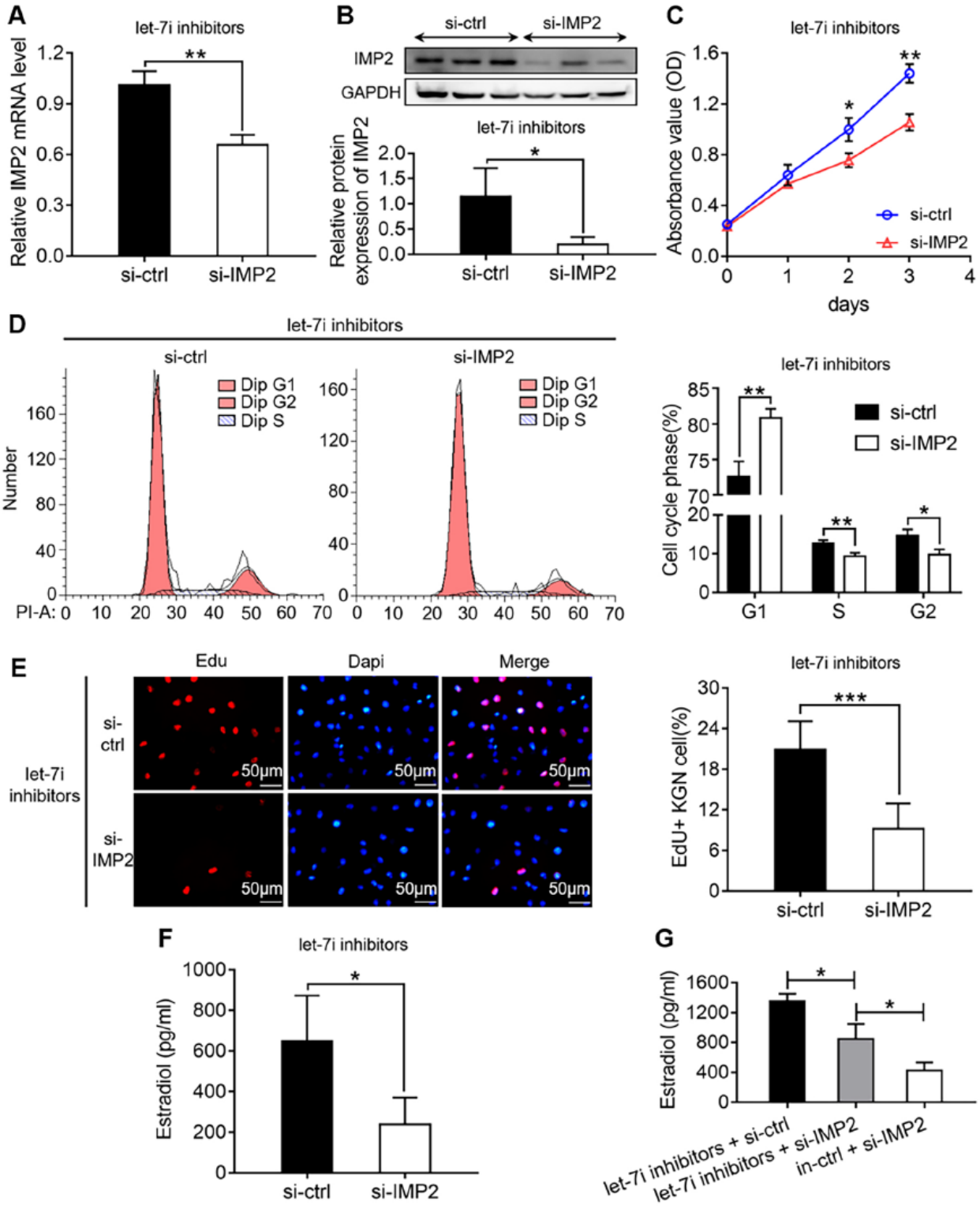

Figure 7

Knockdown of IMP2 abolishes the effect of let-7i inhibitors on cell proliferation and E2 production. (A): The IMP2 mRNA levels in let-7i inhibitors group transfected with a small interfering RNA down-regulating IMP2 (si-IMP2) or control (si-ctrl) were measured by qRT-PCR. (B): Western blot showed the protein expression of IMP2 in let-7i inhibitors group transfected with si-IMP2 or si-ctrl. (C): CCK-8 showed that down-regulated expression of IMP2 reduced the cell viability of let-7i inhibitor group. (D): PI staining and

flow cytometry analysis were performed to detect the effects of si-IMP2 and si-ctrl on cell cycle in let-7i inhibitor group. (E): EdU assay showed that percentage of proliferating cells in let-7i inhibitor group cells transfected with si-IMP2 or si-ctrl. (F-G): In the presence of T (100 nM) and FSK (1 μM), the effect of si-IMP2 on E2 production in let-7i inhibitor group cells. Data are shown as the mean ± SD from at least three independent experiments. *P < 0.05, **P < 0.01, ***P < 0.001.

Supplementary Files

This is a list of supplementary files associated with this preprint. Click to download.

- SupplementaryFig.1.tif
- SupplementaryFig.2.tif
- SupplementaryFig.3.tif
- Table1.pdf
- Table2.pdf